

Spin squeezing in Bose-Einstein condensates: Limits imposed by decoherence and non-zero temperature

Alice Sinatra, Jean-Christophe Dornstetter, and Yvan Castin

Laboratoire Kastler Brossel, Ecole Normale Supérieure, UPMC and CNRS, Paris, France

(Dated: September 13, 2011)

We consider dynamically generated spin squeezing in interacting bimodal condensates. We show that particle losses and non-zero temperature effects in a multimode theory completely change the scaling of the best squeezing for large atom numbers. We present the new scalings and we give approximate analytical expressions for the squeezing in the thermodynamic limit. Besides reviewing our recent theoretical results, we give here a simple physical picture of how decoherence acts to limit the squeezing. We show in particular that under certain conditions the decoherence due to losses and non-zero temperature acts as a simple dephasing.

PACS numbers: 03.75.Gg, 42.50.Dv, 03.75.Mn.

Contents

I. Introduction	1
A. Spin squeezing and atomic clocks	1
B. State of the art	2
C. Two-mode scalings without decoherence	2
D. New scalings in presence of decoherence	3
II. Dephasing Model	3
A. Squeezing in the thermodynamic limit	4
1. Best squeezing and close-to-best time	4
2. Geometrical interpretation	5
B. Exact solution of the dephasing model	5
C. Squeezing in the weak dephasing limit	6
III. Particle losses	6
A. Monte Carlo wave functions	7
B. Losses randomly kick the relative phase	7
C. Spin squeezing limit and the lost fraction	7
D. Analogy between dephasing and losses	8
E. Optimum squeezing in a harmonic trap	9
IV. Finite temperature	9
A. Multimode description	10
B. Best squeezing and close-to-best time	10
C. Spin squeezing and non-condensed fraction	11
V. A few words about experiments	11
VI. Conclusions	11
A. Times t_{\min} and t'_η in the dephasing model	12
B. Calculation of $\langle D^2 \rangle$ in the lossy model	12
References	12

I. INTRODUCTION

Spin squeezing is about creating quantum correlations in a many-body system that can be useful for metrol-

ogy. An example is that of atomic clocks, where the ultimate signal to noise ratio, once all the technical noise has been eliminated, can be improved by manipulating and controlling the system at the level of its quantum fluctuations.

A. Spin squeezing and atomic clocks

The aim of an atomic clock is to measure precisely the energy difference between two atomic states a and b that are for example two hyperfine states of an alkali atom. To explain how the clock works and to introduce spin squeezing, we shall describe the ensemble of N atoms used in the clock using the picture of a “collective spin” that evolves on the so-called Bloch sphere. The collective spin is simply the sum of the effective spins $1/2$ that describe the internal degrees of freedom of each atom. In the second quantized formalism the three hermitian spin components S_x , S_y and S_z are defined by:

$$S_x + iS_y = a^\dagger b, \quad S_z = \frac{a^\dagger a - b^\dagger b}{2}, \quad (1)$$

where a^\dagger and b^\dagger are creation operators of particles in the internal states a and b . The spin operators are dimensionless and obey the commutation relations $[S_x, S_y] = iS_z$ and cyclic permutations. For the moment we do not care about the external degrees of freedom of the atoms. The component S_z of the collective spin is half the population difference between states a and b , while S_x and S_y describe the coherence between these states. If the N atoms are prepared in a coherent superposition of states a and b with relative phase 2ϕ :

$$|\phi\rangle_N = \frac{1}{\sqrt{N!}} \left(\frac{e^{i\phi} a^\dagger + e^{-i\phi} b^\dagger}{\sqrt{2}} \right)^N |0\rangle, \quad (2)$$

where $|0\rangle$ is the vacuum, the collective spin lies on the equatorial plane of the Bloch sphere, pointing at an angle -2ϕ with respect to the x axis. For non-interacting atoms, the further evolution is ruled by the Hamiltonian

$$H_0 = \hbar\omega_{ab} S_z \quad (3)$$

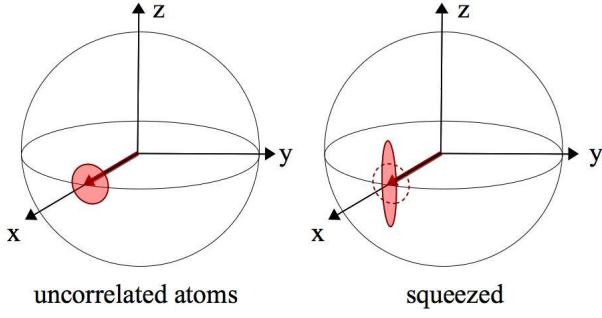


FIG. 1: (Color online) Uncorrelated state and squeezed state represented on the Bloch sphere.

and the spin precesses around the z axis with the Larmor frequency ω_{ab} . The atomic clock measures the phase accumulated by the collective spin during a long precession time τ . From this phase the frequency ω_{ab} is deduced. Atomic clocks are nowadays so precise that they are sensitive to the quantum noise of the collective spin. If for example the spin is initially prepared along the x axis (in an eigenstate of S_x), it has necessarily fluctuations in the transverse components S_y and S_z such that:

$$\langle S_x \rangle = \frac{N}{2}, \quad \Delta S_y \Delta S_z \geq \frac{1}{2} |\langle S_x \rangle|. \quad (4)$$

In particular fluctuations of S_y introduce a statistical variance on the accumulated phase during the precession time and on the measured frequency ω_{ab} . In the uncorrelated state (2) with $\phi = 0$, root mean square fluctuations of S_y and S_z are equal: $\Delta S_y = \Delta S_z = \sqrt{N}/2$. In a Ramsey measurement with interrogation time τ , these quantum fluctuations introduce the root mean square fluctuations of the measured frequency equal to [1]:

$$\Delta \omega_{ab}^{\text{unc}} = \frac{1}{\sqrt{N}\tau}. \quad (5)$$

This noise coming from quantum fluctuations, intrinsic to the initial state where each atom is in a superposition of a and b , is known in clocks as the “partition noise”. The idea of spin squeezing [2] is that the Heisenberg relation (4) allows to reduce ΔS_y provided that ΔS_z is increased. This idea is illustrated in Fig.1. To quantify the spin squeezing we use the parameter ξ^2 introduced in [1]:

$$\xi^2 = \frac{N \Delta S_{\perp, \min}^2}{|\langle \mathbf{S} \rangle|^2} \quad (6)$$

where N is the total atom number, $\Delta S_{\perp, \min}^2$ is the minimal variance of the spin orthogonally to its mean value $\langle \mathbf{S} \rangle$. The state is squeezed if and only if $\xi^2 < 1$. As explained in [1], ξ directly gives the reduction of the statistical fluctuations of the measured frequency ω_{ab} with respect to uncorrelated atoms, for the same atom number N and the same Ramsey time τ :

$$\Delta \omega_{ab}^{\text{sq}} = \xi \Delta \omega_{ab}^{\text{unc}} = \frac{\xi}{\sqrt{N}\tau}. \quad (7)$$

The parameter ξ in Eq.(6) is in fact the properly normalized ratio between the “noise” $\Delta S_{\perp, \min}$ and the “signal” $|\langle \mathbf{S} \rangle|$. In experiments $\Delta S_{\perp, \min}$ is directly measured by measuring S_z after an appropriate state rotation and $|\langle \mathbf{S} \rangle|$ is separately deduced from the Ramsey fringes contrast.

B. State of the art

On one hand the most precise atomic clocks using microwave transitions in cold alkali atoms have already reached the quantum partition noise limit with atom numbers up to $N = 6 \times 10^5$ [3]. On the other hand, very recently a significant amount of spin squeezing, up to -8 dB ($\xi^2 = 10^{-0.8}$) [4] was measured in dedicated, proof-of-principle experiments. In [5] squeezing was created in a large sample of $N = 5 \times 10^4$ atoms with a feedback mechanism in a resonant optical cavity, while in [4] and in [6] the squeezing was created in smaller samples, of order $N = 10^3$, using atomic interactions in bimodal condensates. The ultimate limits of the different paths to spin squeezing are still an open question. Here we concentrate on a dynamical scheme using interactions in bimodal condensates [4, 6–8] and analyze in particular the influence of dephasing, decoherence and non-zero temperature on this squeezing scheme.

C. Two-mode scalings without decoherence

We consider for simplicity a bimodal condensate with identical interactions in the components a and b with coupling constants $g_{aa} = g_{bb} = g$ and no crossed a - b interactions [23]. We assume that the initial state is the factorized state (2) with $\phi = 0$ and a fixed total number of atoms N . In a two-mode picture, interactions introduce a Hamiltonian that is non-linear in the spin operator:

$$H_{\text{nl}} = \hbar \chi S_z^2. \quad (8)$$

The quadratic form (8) is obtained expanding the system Hamiltonian to second order around the average numbers of particles in components a and b , \bar{N}_a and \bar{N}_b , both equal to $N/2$ for the initial state (2) [9, 10]. $\hbar \chi$ is thus the derivative of the chemical potential with respect to the particle number in each component $\hbar \chi = d\mu_a/dN_a = d\mu_b/dN_b$ evaluated in $N_a = \bar{N}_a$, $N_b = \bar{N}_b$. The general expression of the expanded Hamiltonian including drift terms for non-symmetric interactions, non-symmetric splitting or fluctuations in the total particle number can be found in [10, 11]. We are interested in the best squeezing that can be obtained in the thermodynamic limit for a spatially homogeneous system:

$$N \rightarrow \infty, \quad \rho = \frac{N}{V} = \text{constant}, \quad (9)$$

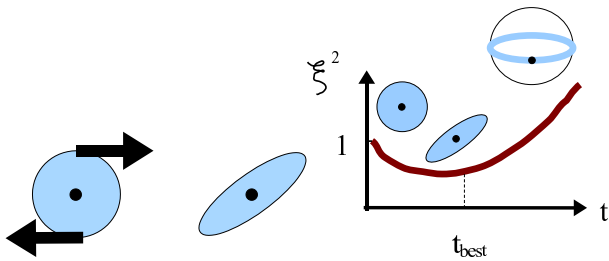


FIG. 2: (Color online) Left: Deformation of quantum fluctuations due to the non-linear Hamiltonian (8). Right: Best squeezing time.

we therefore explicitly write χ in terms of the interaction constant g and the volume V of the system:

$$\mu_a = \frac{gN_a}{V}, \quad \mu_b = \frac{gN_b}{V}, \quad \chi = \frac{g}{\hbar V}. \quad (10)$$

We can consider the non-linear Hamiltonian (8) as a Hamiltonian of the form (3) with a Larmor frequency ω_{ab} that depends itself on S_z . As explained in [2] and shown in Fig.2 (left), H_{nl} “twists” the transverse spin fluctuations and generates spin squeezing. However, in order to minimize ξ^2 , the evolution should not go too far. E.g. when the fluctuations become too much distorted and start to wrap around the Bloch sphere, the “signal” $|\langle \mathbf{S} \rangle|$ in the denominator of ξ^2 decreases and the squeezing parameter increases again. A sketch of the time dependence of ξ^2 when the state (2) evolves under the influence of H_{nl} (8) is given in Fig.2 (right). We name “best squeezing time” t_{min} the time that minimizes $\xi^2(t)$ and “best squeezing” ξ_{min}^2 the corresponding squeezing. The analytical expression for the squeezing as a function of time is given in [2]. Introducing an appropriate rescaling of the time variable as in [12], this gives the following scalings of the best squeezing and the best squeezing time for $N \gg 1$ and ρ, g constants:

$$(\xi_{\text{min}}^2)_{H_{\text{nl}}} \simeq \frac{3^{2/3}}{2} \frac{1}{N^{2/3}}; \quad \left(\frac{\rho g t_{\text{min}}}{\hbar} \right)_{H_{\text{nl}}} \simeq 3^{1/6} N^{1/3}. \quad (11)$$

This differs from the original prediction in [2] by numerical factors. Subsequent studies [7, 13] gave indications that the achievement of large squeezing in condensates should be possible even in presence of decoherence, but were not able to confirm or disprove the scalings (11).

D. New scalings in presence of decoherence

We will show in sections III and IV that the scalings (11) are disproved when decoherence coming from particle losses or non-zero temperature is included in the description. To summarize, instead of tending to zero when $N \rightarrow \infty$ in the thermodynamic limit, ξ_{min}^2 tends to a positive constant

$$\xi_{\text{min}}^2 \xrightarrow{\text{lim. therm.}} \text{constant} > 0. \quad (12)$$

Concerning the best squeezing time t_{min} we distinguish two cases. In the case of particle losses t_{min} is finite in the thermodynamic limit and scales as

$$\frac{\rho g t_{\text{min}}}{\hbar} \propto \frac{1}{\sqrt{\xi_{\text{min}}^2}}. \quad (13)$$

In the case of finite temperature t_{min} cannot be calculated within our analytical treatment that neglects interactions among Bogoliubov modes. Nevertheless, we introduce a “close-to-best” squeezing time t_η defined in equation (37), at which ξ^2 approaches ξ_{min}^2 with a finite precision η , that scales as

$$\frac{\rho g t_\eta}{\hbar} \propto \frac{1}{\sqrt{\eta \xi_{\text{min}}^2}} \quad (14)$$

provided that t_η remains smaller than the typical collision time among Bogoliubov modes.

We will show that these new scalings in presence of decoherence are quite general and that the physics of how decoherence acts is caught by a very simple dephasing model that we shall solve exactly and study in detail in the next section.

II. DEPHASING MODEL

In this section we consider a dephasing Hamiltonian model of the form

$$H = \hbar \chi (S_z^2 + D S_z) \quad (15)$$

where D is a Gaussian real random variable of zero mean. We assume here that D is time independent, but it varies randomly from one experimental realization to the other mimicking a stationary random dephasing environment. We also assume that D has a variance of the order of N for N large [24]:

$$\frac{\langle D^2 \rangle}{N} \rightarrow \epsilon_{\text{noise}}, \quad N \rightarrow \infty. \quad (16)$$

Finally ϵ_{noise} , finite in the thermodynamic limit, is a small parameter of the theory and we limit ourselves in general to first order in this quantity. An exception is made in subsection IIB where expressions to all orders in ϵ_{noise} are given.

Starting with the initial state (2) with $\phi = 0$, we will show that this minimal model reproduces the scalings (12) and (14). In the subsequent sections III and IV we will detail an analogy between the dephasing model and microscopic models accounting for the effect of particle losses or of non-zero temperature on squeezing. The parameter ϵ_{noise} introduced here (16) will then be related to the lost fraction of particles or the populations of thermally excited modes, respectively.

A. Squeezing in the thermodynamic limit

For the symmetric case we consider, the mean spin is always aligned along x . The minimum transverse spin variance is

$$\Delta S_{\perp, \min}^2 = \frac{1}{2} \left[\langle S_y^2 \rangle + \langle S_z^2 \rangle - \sqrt{(\langle S_y^2 \rangle - \langle S_z^2 \rangle)^2 + \langle \{S_z, S_y\} \rangle^2} \right], \quad (17)$$

where the expectation values $\langle \dots \rangle$ represent the average over the quantum state and over the random variable D . The notation $\{, \}$ stands for the anticommutator. Introducing quantities A and B ,

$$A = \langle S_y^2 \rangle - \frac{N}{4} \quad (18)$$

$$B = \langle \{S_z, S_y\} \rangle \quad (19)$$

$$\Delta S_{\perp, \min}^2 = \frac{1}{2} \left[\frac{N}{2} + A - \sqrt{A^2 + B^2} \right]. \quad (20)$$

To derive the scalings (12) and (14), and to have a physical insight, it is convenient to reason in terms of the phases of the operators a and b :

$$a = e^{i\theta_a} \sqrt{N_a} \quad , \quad [N_a, \theta_a] = i \quad (21)$$

$$b = e^{i\theta_b} \sqrt{N_b} \quad , \quad [N_b, \theta_b] = i, \quad (22)$$

where $N_a = a^\dagger a$ and $N_b = b^\dagger b$. This is a legitimate representation as long as the condensate modes have a negligible probability of being empty [14]. By neglecting the fluctuations of their modulus, the collective spin components S_x, S_y are simply given by

$$S_x \simeq \text{Re} \frac{N}{2} e^{-i(\theta_a - \theta_b)}, \quad (23)$$

$$S_y \simeq \text{Im} \frac{N}{2} e^{-i(\theta_a - \theta_b)}. \quad (24)$$

At $t = 0$, the phase difference $(\theta_a - \theta_b)$ has zero mean and root mean square fluctuations that scale as $1/\sqrt{N}$. Both S_y and S_z scale as \sqrt{N} . As a consequence, for N large we can expand the exponentials in (23)-(24). To lowest order we then have

$$S_x \simeq \frac{N}{2}, \quad S_y \simeq -\frac{N}{2}(\theta_a - \theta_b), \quad S_z = \frac{N_a - N_b}{2}. \quad (25)$$

S_y and S_z are then simply proportional to the position operator Q and the momentum operator P of a fictitious free particle. As we will see, the expansions (25) remain valid for times $(\rho g t / \hbar) \ll \sqrt{N}$. The squeezing occurs because in a given realization of the experiment S_y becomes an enlarged copy of S_z . Indeed after the pulse, for $t > 0$, from the Heisenberg equations of motions for the phase operators, with $\chi = g/(\hbar V)$, one has

$$(\theta_a - \theta_b)(t) = (\theta_a - \theta_b)(0^+) - \frac{gt}{\hbar V} [2S_z + D]. \quad (26)$$

As the squeezing dynamics goes on, S_y that was initially of the same order as S_z , grows linearly in time while S_z stays constant. Correspondingly $A \propto t^2$ and $B \propto t$. Since $\langle \{S_y(0), S_z\} \rangle = 0$, one actually has at all times:

$$S_y = S_y(0) + S_y^{\text{lead}} t; \quad (27)$$

$$\frac{A}{N} = \alpha t^2; \quad (28)$$

$$\frac{B}{N} = \beta t, \quad (29)$$

where we have introduced the time independent operator and coefficients

$$S_y^{\text{lead}} = \frac{\rho g}{2\hbar} [2S_z + D] \quad (30)$$

$$\alpha = \frac{\langle (S_y^{\text{lead}})^2 \rangle}{N} = \left(\frac{\rho g}{2\hbar} \right)^2 (1 + \epsilon_{\text{noise}}) \quad (31)$$

$$\beta = \frac{\langle \{S_y^{\text{lead}}, S_z\} \rangle}{N} = \frac{\rho g}{2\hbar}. \quad (32)$$

Using the fact that from (25) $S_x \simeq N/2$ for $(\rho g t / \hbar) \ll \sqrt{N}$, and expanding the expression (20) for $t \gg \hbar/(\rho g)$, we have in the thermodynamic limit

$$\xi^2(t) \xrightarrow{t \rightarrow \infty} 1 - \frac{\beta^2}{\alpha} + \frac{\beta^4}{4\alpha^3} \frac{1}{t^2} + O(t^{-4}). \quad (33)$$

Using equations (30)-(32), with $\epsilon_{\text{noise}} \ll 1$, we finally obtain in the long time limit

$$\xi^2(t) = \epsilon_{\text{noise}} + \left(\frac{\hbar}{\rho g t} \right)^2 [1 + O(\epsilon_{\text{noise}})] + O\left(\frac{\hbar^4}{(\rho g t)^4} \right). \quad (34)$$

1. Best squeezing and close-to-best time

According to (34), the best squeezing in the thermodynamic limit to leading order in ϵ_{noise} is

$$\xi_{\min}^2 = \epsilon_{\text{noise}} = \lim_{N \rightarrow \infty} \frac{\langle D^2 \rangle}{N}. \quad (35)$$

Remarkably, the best squeezing (35) only involves the part of the phase difference D that is not proportional to S_z . To understand physically this result we rewrite

$$\xi_{\min}^2 = 1 - \frac{\beta^2}{\alpha} = \frac{\langle (S_y^{\text{lead}})^2 \rangle \langle S_z^2 \rangle - \langle \{S_y^{\text{lead}}, S_z\} / 2 \rangle^2}{\langle (S_y^{\text{lead}})^2 \rangle \langle S_z^2 \rangle}. \quad (36)$$

Due to interactions, through the phase difference (26), S_y^{lead} is proportional to $(2S_z + D)$. In the absence of the term D this allows a perfect cancellation between the correlation $\langle S_y^{\text{lead}} S_z \rangle^2$ and the product $\langle (S_y^{\text{lead}})^2 \rangle \langle S_z^2 \rangle$ in (36) leading to $\xi_{\min}^2 = 0$ in the limit $N \rightarrow \infty$. In presence of D , this is not possible and ξ_{\min}^2 has a non-zero limit.

Considering the next to leading order in the time expansion of the squeezing parameter Eq.(34), the best

squeezing is reached in an infinite time (in the thermodynamic limit). However as we will see $\xi^2(t)$ is quite flat around its minimum, and it suffices to determine a “close-to-best” squeezing time t_η defined as

$$\xi^2(t_\eta) = (1 + \eta)\xi_{\min}^2, \quad \eta > 0. \quad (37)$$

Then, according to (34), t_η is given by

$$\frac{\rho g}{\hbar} t_\eta = \frac{1}{\sqrt{\eta \xi_{\min}^2}}. \quad (38)$$

The close-to-best squeezing time t_η is thus very simply related to the best squeezing ξ_{\min}^2 . The important point is that t_η is finite (non-infinite and non-zero) in the thermodynamic limit.

2. Geometrical interpretation

We give here a geometrical and pictorial interpretation to the squeezing process in the thermodynamic limit. Let us introduce the rescaled transverse spin components

$$Y = \frac{S_y}{\sqrt{\langle S_y^2 \rangle}}, \quad Z = \frac{S_z}{\sqrt{\langle S_z^2 \rangle}} \quad (39)$$

that verify $\langle Y \rangle = \langle Z \rangle = 0$ and $\langle Y^2 \rangle = \langle Z^2 \rangle = 1$. At short times, the Wigner function representing the probability distribution of Y and Z is approximately Gaussian

$$W(y, z) \propto \exp \left[-\frac{1}{2} (y, z) M^{-1} \begin{pmatrix} y \\ z \end{pmatrix} \right] \quad (40)$$

where M is the covariance matrix

$$M = \begin{pmatrix} \langle Y^2 \rangle & \frac{1}{2} \langle \{Y, Z\} \rangle \\ \frac{1}{2} \langle \{Y, Z\} \rangle & \langle Z^2 \rangle \end{pmatrix}. \quad (41)$$

We can represent graphically the fluctuations of Y and Z by drawing isocontours of $W(y, z)$. Let us introduce the eigenvalues of M

$$\lambda_{1,2} = 1 \pm \frac{1}{2} \langle \{Y, Z\} \rangle. \quad (42)$$

and a rotated coordinate system $y' - z'$ aligned with the eigenvectors of M :

$$y' = (z + y)/\sqrt{2}; \quad z' = (z - y)/\sqrt{2}. \quad (43)$$

The points in the $y'z'$ plane such that

$$\frac{y'^2}{\lambda_1} + \frac{z'^2}{\lambda_2} = 1 \quad (44)$$

form an ellipse whose semi-axis gives the mean square fluctuations of Y' and Z' that are time dependent linear combinations of S_y and S_z . The ellipse surface $\mathcal{S}_{\text{ellipse}} = \pi(\lambda_1 \lambda_2)^{1/2}$ divided by π is equal to the square root of the

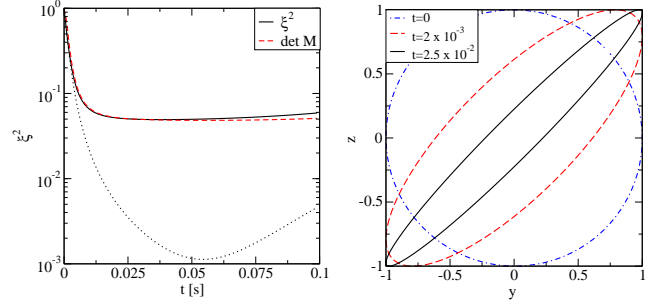


FIG. 3: (Color online) Left: Squeezing parameter ξ^2 as a function of time for $\epsilon_{\text{noise}} = 0.05$ (full line) and $\epsilon_{\text{noise}} = 0$ (dotted line). Determinant of the covariance matrix M as a function of time (dashed line). Simulation with 10^4 realizations. $N = 4 \times 10^4$, $\chi = 0.022577\text{s}^{-1}$. Right: Isocontours of $W(y, z)$ for $t = 0$, $t = 2 \times 10^{-3}$ s and $t = 2.5 \times 10^{-2}$ s.

determinant of M and is thus asymptotically equivalent to ξ_{\min} according to (36):

$$\xi_{\min} = \frac{\mathcal{S}_{\text{ellipse}}}{\pi} \quad \text{for } t \gg \frac{\hbar}{\rho g}. \quad (45)$$

In Fig.3 (left) we show the time dependence of the squeezing parameter ξ^2 in presence and in absence of decoherence. On the same plot we show the determinant of M that asymptotically gives the value of ξ_{\min}^2 (36). In Fig.3 (right) we show the isocontours of $W(y, z)$ defined by (44) at different times for the case with decoherence. As the dynamics goes on, Y and Z become more and more correlated and the ellipse shrinks. In the absence of dephasing and in the thermodynamic limit the ellipse would collapse into a segment in the $y = z$ direction. In the presence of decoherence the process is “blocked” and the ellipse keeps a finite width with a limit area $\mathcal{S}_{\text{ellipse}} = \pi \epsilon_{\text{noise}}$.

B. Exact solution of the dephasing model

The dephasing model (15) is exactly solvable. One first writes the Heisenberg equations of motion for a and b , e.g.

$$i \dot{a} = \frac{\chi}{2} \left(2S_z + D + \frac{1}{2} \right) a. \quad (46)$$

Then one uses the fact that S_z is a constant of motion to integrate the equations [10, 15]. One obtains (see also [16]):

$$\xi^2(t) = \frac{\frac{N}{2} \left[\frac{N}{2} + A - \sqrt{A^2 + B^2} \right]}{C^2} \quad (47)$$

with

$$A = \frac{N(N-1)}{8} \left[1 - e^{-2(\chi t)^2 \langle D^2 \rangle} (\cos 2\chi t)^{N-2} \right] \quad (48)$$

$$B = \frac{N(N-1)}{2} \sin \chi t e^{-\frac{1}{2}(\chi t)^2 \langle D^2 \rangle} (\cos \chi t)^{N-2} \quad (49)$$

$$C = \langle S_x \rangle = \frac{N}{2} e^{-\frac{1}{2}(\chi t)^2 \langle D^2 \rangle} (\cos \chi t)^{N-1}. \quad (50)$$

A first application of the exact solution (47)-(50) is to determine the best squeezing ξ_{\min}^2 in the thermodynamic limit, to all orders in the dephasing parameter ϵ_{noise} . To this aim we take the limit $N \rightarrow \infty$ in (47)-(50) at fixed time t , density ρ and noise parameter $\epsilon_{\text{noise}} = \langle D^2 \rangle / N$. We find that A/N , B/N and C/N have a finite limit and that

$$\xi^2(t) \xrightarrow{\text{lim.therm.}} 1 - \left[\frac{1}{2} (1 + \epsilon_{\text{noise}}) + \sqrt{\frac{1}{4} (1 + \epsilon_{\text{noise}})^2 + \left(\frac{\hbar}{\rho g t} \right)^2} \right]^{-1}. \quad (51)$$

From this solution one gets the best squeezing and the close-to-best squeezing time t_η (for $\eta \epsilon_{\text{noise}} < 1$):

$$\xi_{\min}^2 \xrightarrow{\text{lim.therm.}} \frac{\epsilon_{\text{noise}}}{1 + \epsilon_{\text{noise}}} \quad (52)$$

$$\frac{\rho g}{\hbar} t_\eta \xrightarrow{\text{lim.therm.}} \frac{1 - \eta \epsilon_{\text{noise}}}{(1 + \epsilon_{\text{noise}}) \sqrt{\eta \epsilon_{\text{noise}}}}. \quad (53)$$

Note that one can obtain (35) and (38) from (52) and (53) by linearizing for small ϵ_{noise} .

In Fig.4 we show $\xi^2(t)$ as a function of time for a large atom number. The curve is indeed quite flat around the best squeezing time t_{\min} . There are two solutions to equation (37): $t_\eta < t_{\min}$ and $t'_\eta > t_{\min}$. When $N \rightarrow \infty$, t_η is finite and given by (53). On the other hand, as we show in Appendix A, t_{\min} diverges as $N^{1/4}$ and t'_η diverges as $N^{1/2}$. Knowing the asymptotic behavior of t_{\min} , by introducing appropriate rescalings of the time variable as in [12], it is also possible to obtain the first finite size correction to ξ_{\min}^2 . This is given in equation (A4) of Appendix A.

C. Squeezing in the weak dephasing limit

We can use the exact solution of the dephasing model (47)-(50) to investigate the weak dephasing limit that we define as the limit where the noise D remains bounded for $N \rightarrow \infty$ (see the footnote before equation (16)):

$$\langle D^2 \rangle \rightarrow \text{constant} \quad N \rightarrow \infty. \quad (54)$$

In this case the scaling of the best squeezing time with N is still given by $\rho g t_{\min} / \hbar \propto N^{1/3}$ as in the case without decoherence (11) and, using the same rescaling of time as in [12], one has

$$\xi_{\min}^2 = \frac{3^{2/3}}{2} \frac{1}{N^{2/3}} + \frac{\frac{3}{2} + \langle D^2 \rangle}{N} + o\left(\frac{1}{N}\right), \quad (55)$$

$$\frac{\rho g t_{\min}}{\hbar} = 3^{1/6} N^{1/3} - \frac{\sqrt{3}}{4} + o(1). \quad (56)$$

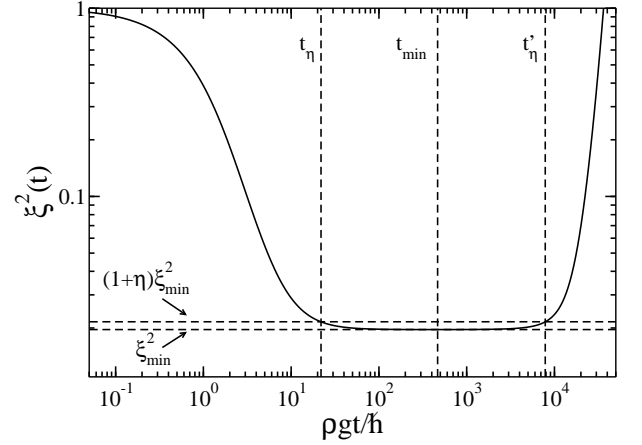


FIG. 4: Squeezing as a function of time for the dephasing model (15) as given by the exact solution (47). $N = 10^9$, $\langle D^2 \rangle / N = 0.02$. Horizontal dashed lines: ξ_{\min}^2 given by (A4) and $(1 + \eta)\xi_{\min}^2$ with $\eta = 0.1$. Vertical dashed lines from left to right: Close-to-best squeezing time t_η (53), best squeezing time t_{\min} (A3) and t'_η deduced from (A5).

III. PARTICLE LOSSES

In this section we consider particle losses that are an intrinsic source of decoherence in condensed gases. Among those, one-body losses are due to collisions of condensate atoms with residual hot atoms due to imperfect vacuum. More fundamental in dense samples are three-body losses where, after a three-body collision, two atoms form a molecule and the third atom takes away the energy to fulfill energy and momentum conservation. After such a collision event the three atoms are lost. Three-body losses are present due to the metastable nature of ultra cold gases, whose real ground state at such low temperatures would be a solid and whose gaseous phase is maintained because the sample is very dilute. Finally two-body losses can also be present, caused by two-body collisions that change the internal state of the atoms. For a trapped gas, we have shown theoretically [12] that the best achievable squeezing within a two-mode model at zero temperature in presence of one, two and three-body losses can in principle be very large (squeezing parameter ξ^2 of the order of 10^{-4}) provided that the harmonic trapping potential is optimized and a careful choice of the internal state of the atoms is made. To realize such conditions that minimize losses remains however an experimental challenge.

In this section we recall the main results of [12] concerning the squeezing in presence of particle losses, and we use these results to show an analogy between the effect of the losses and the effect of the dephasing Hamiltonian (15) in the thermodynamic limit.

A. Monte Carlo wave functions

We consider two spatially separated, symmetric condensates. For a more general treatment, please refer to [11]. Initially the system is in the eigenstate of S_x with maximal eigenvalue $N/2$. Besides the non-linear Hamiltonian for the two bosonic modes a and b given by

$$H_{\text{nl}} = \hbar \chi S_z^2 \quad \text{with} \quad \chi = (\partial_{N_a} \mu_a)_{\bar{N}_a} / \hbar, \quad (57)$$

we include one, two and three-body losses. Due to the losses, the system is “open” and we shall describe it with a density operator that obeys a Master Equation of the Lindblad form [10]. In the interaction picture with respect to H_{nl} :

$$\frac{d\tilde{\rho}}{dt} = \sum_{m=1}^3 \sum_{\epsilon=a,b} \gamma^{(m)} \left[c_\epsilon^m \tilde{\rho} c_\epsilon^{\dagger m} - \frac{1}{2} \{ c_\epsilon^{\dagger m} c_\epsilon^m, \tilde{\rho} \} \right] \quad (58)$$

where $c_\epsilon = \tilde{a}, \tilde{b}$ for $\epsilon = a, b$ and:

$$\tilde{a} = e^{\frac{i}{\hbar} H_{\text{nl}} t} a e^{-\frac{i}{\hbar} H_{\text{nl}} t}; \quad \tilde{b} = e^{\frac{i}{\hbar} H_{\text{nl}} t} b e^{-\frac{i}{\hbar} H_{\text{nl}} t}. \quad (59)$$

Here the operators a and b are in the Schrödinger picture. The m -body loss rates $\gamma^{(m)}$ are defined in terms of the so-called rate constants K_m as

$$\gamma^{(m)} = \frac{K_m}{m} \int d^3 r |\phi(\mathbf{r})|^{2m} \quad (60)$$

where $\phi(\mathbf{r})$ is the condensate wave function in mode a or b for the initial atom number (weak loss approximation), so that for example:

$$\frac{d}{dt} \langle N_a \rangle = - \left\langle \left[K_1 + K_2 N_a \int d^3 r |\phi(r)|^4 + K_3 N_a^2 \int d^3 r |\phi(\mathbf{r})|^6 \right] N_a \right\rangle. \quad (61)$$

It is convenient to rephrase the Master Equation (58) in terms of Monte Carlo wave functions [17]. In this picture pure states evolve deterministically under the influence of an effective Hamiltonian H_{eff} acting during time intervals $\tau_i = t_i - t_{i-1}$ separated by random quantum jumps (described by the jump operators S_ϵ) occurring at times t_i as illustrated in Fig.5:

$$H_{\text{eff}} = - \sum_{\epsilon=a,b} \frac{i\hbar}{2} \gamma^{(m)} c_\epsilon^{\dagger m} c_\epsilon^m, \quad S_\epsilon = \sqrt{\gamma^{(m)}} c_\epsilon^m. \quad (62)$$

More precisely the evolution of the non-normalized state vector $|\psi(t)\rangle$ in between quantum jumps is given by

$$i\hbar \frac{d}{dt} |\psi(t)\rangle = H_{\text{eff}}(t) |\psi(t)\rangle \quad (63)$$

and the effect of a quantum jump in the component ϵ_i at time t_i is

$$|\psi(t_i^+)\rangle = S_{\epsilon_i}(t_i) |\psi(t_i^-)\rangle. \quad (64)$$

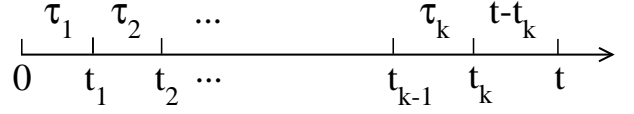


FIG. 5: Time sequence of deterministic evolution periods and quantum jumps for a single Monte Carlo wave function $|\psi\rangle$.

Quantum averages of any atomic observables \mathcal{O} are obtained by summing over all the possible trajectories of the non-normalized state vector [12]:

$$\langle \hat{\mathcal{O}} \rangle = \sum_k \int_{0 < t_1 < t_2 < \dots < t_k} dt_1 dt_2 \dots dt_k \sum_{\{\epsilon_j\}} \langle \psi(t) | \hat{\mathcal{O}} | \psi(t) \rangle. \quad (65)$$

B. Losses randomly kick the relative phase

Let us consider the action of a quantum jump over a phase state (2) with N atoms, for example the loss of one particle in state a or b at time t :

$$c_a(t) |\phi\rangle_N = \sqrt{\frac{N}{2}} e^{-i\frac{\chi}{4}t} e^{i\phi} |\phi - \chi t/2\rangle_{N-1} \quad (66)$$

$$c_b(t) |\phi\rangle_N = \sqrt{\frac{N}{2}} e^{-i\frac{\chi}{4}t} e^{-i\phi} |\phi + \chi t/2\rangle_{N-1}. \quad (67)$$

Under the action of a jump a phase state remains a phase state. On the other hand, the relative phase is shifted by a random amount that depends on the time of the jump and has a random sign depending on whether the jump was in a or b . This behavior is illustrated in Fig.6 taken from [10] where we plot the modulus squared of a relative phase distribution amplitude $c(\phi, t)$ at $t = 0$ and $t = 2\pi/\chi$ for three single Monte Carlo realizations. At this particular time (second revival time) the coherent evolution due to H_{nl} has no effect and we can isolate the action of the losses. In the case of Fig.6, as χt is of the order of unity, the shift in the relative phase due a single jump is large. In the case of squeezing with $N \gg 1$, $\chi t \ll 1$, the shifts due to single quantum jumps are on the contrary very small. These shifts nevertheless limit the maximum squeezing achievable as we shall see.

C. Spin squeezing limit and the lost fraction

Let us consider the case of one-body losses only with a loss rate constant γ equal in states a and b . In this case the effective Hamiltonian does not depend on time; referring to the time sequence in Fig.5, we have explicitly

$$|\psi(t)\rangle = e^{-iH_{\text{eff}}(t-t_k)/\hbar} S_{\epsilon_k}(t_k) e^{-iH_{\text{eff}}\tau_k/\hbar} S_{\epsilon_{k-1}}(t_{k-1}) \dots S_{\epsilon_1}(t_1) e^{-iH_{\text{eff}}\tau_1/\hbar} |\psi(0)\rangle, \quad (68)$$

and there is an explicit analytical solution for the generated spin squeezing as a function of time [11, 12]. Here

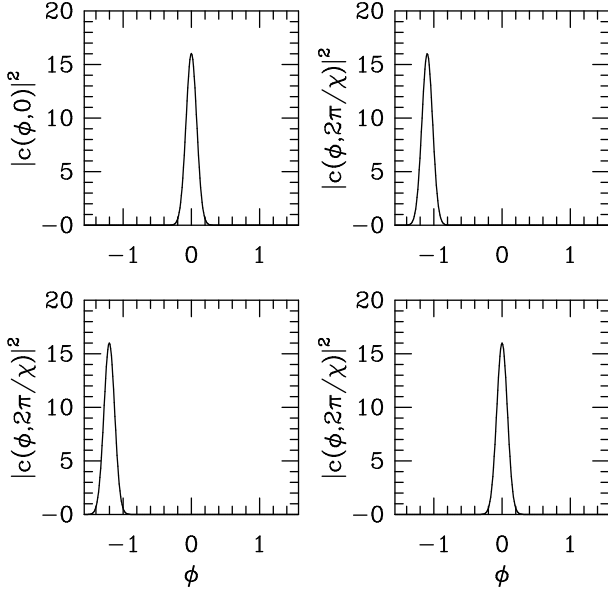


FIG. 6: Relative phase probability distribution at time $t = 0$ and at time $t = 2\pi/\chi$ in three single realizations Monte Carlo realization. From upper left to lower right the wave function has experienced 0, 3, 1 and 0 quantum jumps respectively. Three-body losses corresponding to $N = 301$ ^{87}Rb atoms in $F = 1, m_f = -1$ state in separated identical harmonic traps with $\omega = 500\text{Hz}$. Figure taken from [10].

we use this solution to find the best squeezing in presence of losses in the thermodynamic limit with $N \rightarrow \infty$, ρ and γ constant. For simplicity we also assume that the fraction of lost particles at the relevant time t remains small in the thermodynamic limit:

$$\gamma t \equiv \epsilon_{\text{loss}}. \quad (69)$$

We proceed similarly as we did to derive Eq.(51), taking the thermodynamic limit in the exact solution in presence of losses. Restricting for simplicity to the leading order in γt and to the case $\rho g t / \hbar \gg 1$, we obtain

$$\frac{A}{N e^{-\gamma t}} \simeq \left(\frac{\rho g t}{2\hbar} \right)^2 \left(1 - \frac{5}{3} \gamma t \right) \quad (70)$$

$$\frac{B}{N e^{-\gamma t}} \simeq \frac{\rho g t}{2\hbar} (1 - \gamma t) \quad (71)$$

$$\xi^2(t) \simeq \frac{\gamma t}{3} + \left(\frac{\hbar}{\rho g t} \right)^2 [1 + O(\gamma t)], \quad (72)$$

where A and B are defined in (18)-(19). Equation (72) shows that for long times, the squeezing parameter is asymptotically equivalent to one third of the lost fraction of atoms. Minimizing (72) with respect to time we obtain

$$\xi_{\min}^2 = \frac{3}{4} \left(\frac{4\hbar\gamma}{3\rho g} \right)^{2/3} \quad (73)$$

$$\frac{\rho g}{\hbar} t_{\min} = \left(\frac{3\rho g}{4\hbar\gamma} \right)^{1/3}. \quad (74)$$

In Fig.7 we show the squeezing in presence of losses and we compare the exact solution [12] with the approximate expression (72) valid at long times and in thermodynamic limit.

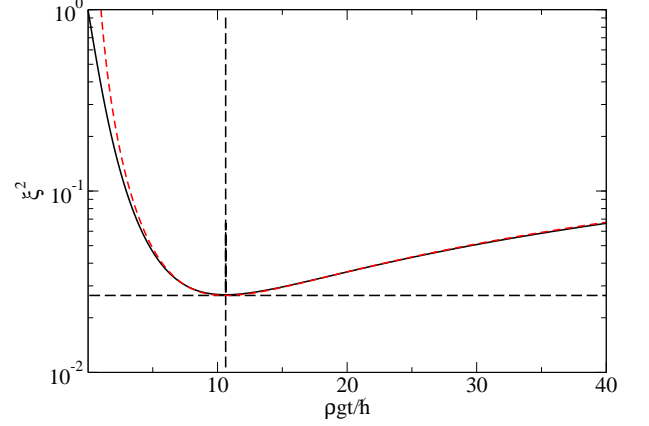


FIG. 7: (Color online) Spin squeezing as a function of time in presence of one-body losses: $\gamma = 0.005\rho g/\hbar$, $N = 10^6$. Solid black line: Exact analytical solution. Dashed red line: Approximate solution (72). Horizontal and vertical dashed lines: predictions (73) and (74) respectively.

D. Analogy between dephasing and losses

Our goal here is to make an analogy between the dephasing model of section II and the present model with losses. Indeed the relative phase is perturbed by the losses. In presence of one-body losses, a non normalized Monte Carlo wave function after k jumps has the form:

$$|\psi(t)\rangle = \mathcal{N}^{1/2} e^{i\tilde{\phi}} |\phi + \frac{\chi t}{2} \mathcal{D}\rangle_{N-k}, \quad (75)$$

$$\mathcal{N} = \left(\prod_{i=1}^k e^{-\gamma t_i} \right) e^{-\gamma(N-k)t} \gamma^k \times \frac{N(N-1)\dots(N-k+1)}{2^k}, \quad (76)$$

$$\mathcal{D} = \frac{1}{t} \sum_{l=1}^k t_l (\delta_{\epsilon_l, b} - \delta_{\epsilon_l, a}). \quad (77)$$

The factor \mathcal{N} given by (76) is the norm squared of the wave function that is needed to calculate quantum averages, the first line in (76) is due to the effective Hamiltonian evolution, $\tilde{\phi}$ is an irrelevant phase and \mathcal{D} given by (77) is a random perturbation of the relative phase 2ϕ that plays the role of the quantity D in Eq.(26) of the dephasing model of section II, as appears from the fact that $\exp(-i\chi t D S_z) |\phi\rangle_N = |\phi - \chi t D/2\rangle_N$. Contrarily to D , \mathcal{D} given by (77) is time dependent. As detailed in Appendix B, using (65) we can calculate $\langle \mathcal{D}^2 \rangle$. To first

order in γt we obtain:

$$\frac{\langle \mathcal{D}^2 \rangle}{N} \simeq \frac{\gamma t}{3}. \quad (78)$$

We have thus shown that $\xi^2(t)$ is asymptotically equivalent to $\langle \mathcal{D}^2 \rangle / N$ as it the case in the dephasing model. We can then establish an analogy between the model with losses and the dephasing model as summarized in the first two columns of the Table I. In Fig.8 we show a comparison of $\langle \mathcal{D}^2 \rangle / N$ obtained from a Monte Carlo simulation, from the exact expression (B7), and from the approximate expression (78) valid to first order in $\epsilon_{\text{loss}} = \gamma t$.

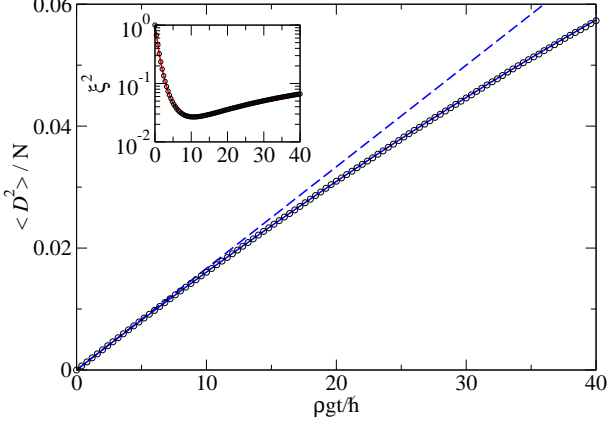


FIG. 8: (Color online) Main plot: $\langle \mathcal{D}^2 \rangle / N$ given by (77) as a function of time for $\gamma = 0.005 \rho g / \hbar$, $N = 10^6$. Black circles: Numerical simulation with 5×10^5 realizations. Dashed blue line: Approximate expression (78). Solid blue line: Exact expression (B7). Inset: Squeezing as a function of time. Solid red line: Exact analytical solution. Black circles: Numerical simulation with 5×10^5 realizations.

E. Optimum squeezing in a harmonic trap

A similar analysis can be performed for a trapped system, where we now consider the two components a and b in identical and spatially separated harmonic traps. In particular equation (19) of [12] is very similar to (72) except that in (19) of [12] we have $N\chi$ instead of ρg in (72). Another difference is that the more general equation (19) in [12] that includes two and three-body losses besides one-body losses, is derived performing an approximation on the effective Hamiltonian: the constant loss rate approximation [25]

$$H_{\text{eff}} = - \sum_{\epsilon=a,b} \frac{i\hbar}{2} \gamma^{(m)} c_{\epsilon}^{\dagger m} c_{\epsilon}^m \simeq - \sum_{\epsilon=a,b} \frac{i\hbar}{2} \gamma^{(m)} \bar{N}_{\epsilon}^m. \quad (79)$$

By using (19) of [12] and the Thomas-Fermi profiles of the condensate wave functions, one can optimize the squeezing with respect to time, trap frequency and atom

number. This optimum squeezing in a trap in presence of one, two and three-body losses has a simple expression as a function of the s -wave scattering length $a_{aa} = a_{bb} = a$ and the rate constants K_m , $m = 1, 2, 3$:

$$\xi_{\text{opt}}^2 = \left(\frac{5\sqrt{3}}{28\pi} \frac{M}{\hbar a} \right)^{2/3} \left[\sqrt{\frac{7}{2} (K_1 K_3) + K_2} \right]^{2/3}. \quad (80)$$

In Fig.9 we show the spin squeezing minimized over time ξ_{min}^2 as a function of N in presence of one, two and three-body losses. The trap frequency is optimized for each value of N [12]:

$$\omega_{\text{opt}} = \frac{2^{19/12} 7^{5/12} \pi^{5/6}}{15^{1/3}} \frac{\hbar}{m} \frac{a^{1/2}}{N^{1/3}} \left(\frac{K_1}{K_3} \right)^{5/12}. \quad (81)$$

We note that the minimum squeezing, instead of going to zero as in two-mode model without decoherence (red line) tends to a finite non-zero value for $N \rightarrow \infty$ given by (80).

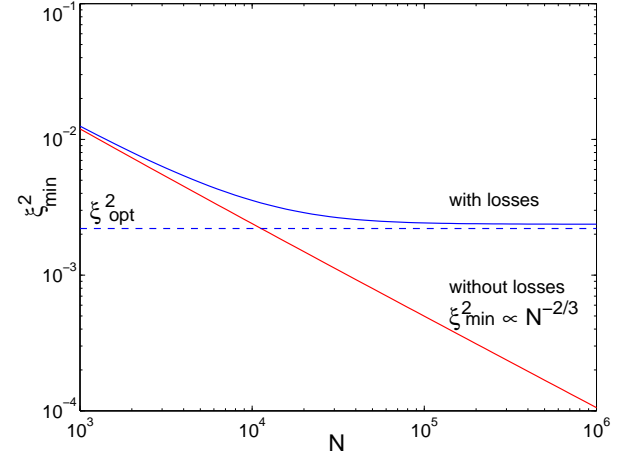


FIG. 9: (Color online) Blue line: Best squeezing ξ_{min}^2 as a function of N in presence of one, two and three-body losses, obtained in [12] in the constant loss rate approximation. The trap frequency is optimized for each value of N according to (81). Dashed blue line: Optimum squeezing for large N given by the analytical prediction (80). Red line: Best squeezing without losses for comparison. Parameters: $a = 5.32 \text{ nm}$, $K^{(1)} = 0.1 \text{ s}^{-1}$, $K^{(2)} = 2 \times 10^{-21} \text{ m}^3 \text{ s}^{-1}$, $K^{(3)} = 18 \times 10^{-42} \text{ m}^6 \text{ s}^{-1}$. This figure is taken from [18].

IV. FINITE TEMPERATURE

The multimode nature of the atomic field and the population in the excited modes at non-zero temperature have important consequences on the squeezing and change the scaling laws with respect to the two-mode case (11). In [19] we use a powerful formulation of the Bogoliubov theory in terms of the time dependent condensate phase operator [20, 21] to perform a multimode

treatment of the squeezing generation in a condensed gas in the homogeneous case. We show that the best squeezing ξ_{\min} has a finite non-zero value in the thermodynamic limit and we calculate this value analytically.

A. Multimode description

We consider a discretized model on a lattice with unit cell of volume dV , within a volume V with periodic boundary conditions [21]. The Hamiltonian after the pulse for component a (and similarly for b) reads:

$$H_a = \sum_{\mathbf{k}} \frac{\hbar^2 k^2}{2m} a_{\mathbf{k}}^\dagger a_{\mathbf{k}} + \frac{g}{2} dV \sum_{\mathbf{r}} \psi_a^\dagger(\mathbf{r}) \psi_a^\dagger(\mathbf{r}) \psi_a(\mathbf{r}) \psi_a(\mathbf{r}). \quad (82)$$

The fields have commutators

$$[\psi_\mu(\mathbf{r}), \psi_\nu^\dagger(\mathbf{r}')] = \frac{\delta_{\mathbf{r}\mathbf{r}'} \delta_{\mu\nu}}{dV} \quad (83)$$

with $\mu, \nu = a$ or b , and $a_{\mathbf{k}}(b_{\mathbf{k}})$ is the amplitude of $\psi_{a,b}$ over the plane wave of momentum \mathbf{k} . We assume identical interactions in states a and b with a coupling constant $g = 4\pi\hbar^2 a/m$ where a is the s -wave scattering length while states a and b do not interact ($g_{ab} = 0$). Note that the coupling constant in $H_{a,b}$ should actually be a bare coupling constant g_0 different from the effective coupling constant g , but this difference can be made small in the present weakly interacting regime $(\rho a^3)^{1/2} \ll 1$ by choosing a lattice spacing much larger than a but still much smaller than the healing length $\propto 1/\sqrt{\rho a}$ [22].

In terms of the fields, the collective spin components are

$$S_x + iS_y = dV \sum_{\mathbf{r}} \psi_a^\dagger(\mathbf{r}) \psi_b(\mathbf{r}), \quad S_z = \frac{N_a - N_b}{2} \quad (84)$$

with $N_\nu = dV \sum_{\mathbf{r}} \psi_\nu^\dagger(\mathbf{r}) \psi_\nu(\mathbf{r})$, $\nu = a, b$.

For low or high values of $k_B T / \rho g$ we find the asymptotic behaviors

$$k_B T \ll \rho g : \quad \frac{\xi_{\min}^2}{\sqrt{\rho a^3}} \simeq \frac{\xi_{\min}^2(T=0)}{\sqrt{\rho a^3}} = 0.0234 \dots \quad (85)$$

$$k_B T \gg \rho g : \quad \xi_{\min}^2 \simeq \frac{\langle N_{\text{nc}} \rangle}{N}. \quad (86)$$

B. Best squeezing and close-to-best time

Performing a double expansion for large N and small non-condensed fraction ϵ_{Bog} ,

$$\epsilon_{\text{Bog}} \equiv \frac{\langle N_{\text{nc}} \rangle}{N} \ll 1 \quad (87)$$

we find that to first order the system effectively behaves as in the dephasing model presented in section II. Indeed the component S_y of the spin develops a term that is

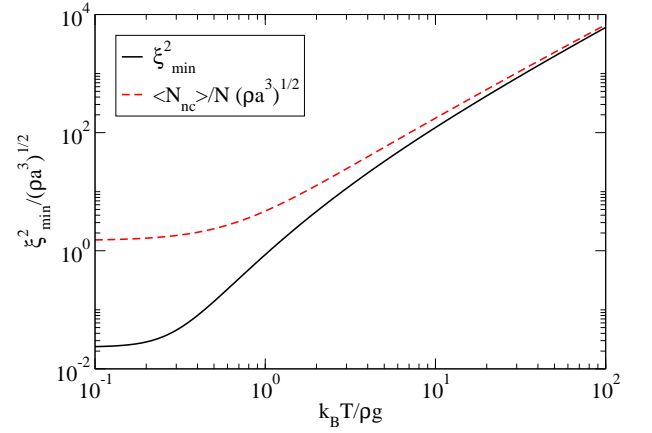


FIG. 10: (Color online) ξ_{\min}^2 (solid line) and before-pulse non-condensed fraction $\langle N_{\text{nc}} \rangle / N$ (dashed line), both divided by $\sqrt{\rho a^3}$, as functions of $k_B T / \rho g$. Both quantities are obtained analytically within a Bogoliubov framework, see (92) for ξ_{\min}^2 .

proportional to the condensate relative phase $\theta_a - \theta_b$, and the relative phase evolves as

$$\theta_a - \theta_b = (\theta_a - \theta_b)(0^+) - \frac{gt}{\hbar V} [(N_a - N_b) + D_{\text{th}}]. \quad (88)$$

The dephasing parameter D_{th} in (88) is related to the population in the excited modes:

$$D_{\text{th}} = \sum_{\mathbf{k} \neq 0} (U_{\mathbf{k}} + V_{\mathbf{k}})^2 (n_{\mathbf{a}\mathbf{k}} - n_{\mathbf{b}\mathbf{k}}), \quad (89)$$

where $n_{\mathbf{a}\mathbf{k}} = c_{\mathbf{a}\mathbf{k}}^\dagger c_{\mathbf{a}\mathbf{k}}$ and $n_{\mathbf{b}\mathbf{k}} = c_{\mathbf{b}\mathbf{k}}^\dagger c_{\mathbf{b}\mathbf{k}}$ are the occupation number operators of the Bogoliubov modes. Note that these modes are in a *non-equilibrium* state since the zero relative phase state between the condensates in a and b is prepared at $t = 0^+$ by applying a sudden $\pi/2$ pulse to the gas (that was initially at thermal equilibrium in state a). $U_{\mathbf{k}}$ and $V_{\mathbf{k}}$ are the usual Bogoliubov functions

$$U_{\mathbf{k}} + V_{\mathbf{k}} = \left(\frac{E_{\mathbf{k}}}{E_{\mathbf{k}} + \rho g} \right)^{1/4}; \quad E_{\mathbf{k}} = \frac{\hbar^2 k^2}{2m}, \quad (90)$$

$\rho/2 = N/2V$ being the spatial density in each single component a or b after the pulse. D_{th} fluctuates from one realization to the other because $n_{\mathbf{a}\mathbf{k}}$ and $n_{\mathbf{b}\mathbf{k}}$ depend (in Heisenberg picture) on the creation and annihilation operators of the Bogoliubov modes before the pulse, and the initial state of the gas has thermal fluctuations.

To first order in N and in ϵ_{Bog} , the best squeezing parameter and the close-to-best squeezing time are given by [19]

$$\xi_{\min}^2 = \frac{\langle D_{\text{th}}^2 \rangle}{N}; \quad \frac{\rho g t_{\eta}}{\hbar} = \frac{1}{\sqrt{\eta \xi_{\min}}}. \quad (91)$$

An explicit calculation [19] gives:

$$\xi_{\min}^2 = \int \frac{d^3 k}{(2\pi)^3} \frac{s_k^4}{2\rho} \left[\left(n_k^{(0)} + \frac{1}{2} \right) \left(\frac{(s_k^{(0)})^2}{s_k^4} + \frac{s_k^4}{(s_k^{(0)})^2} \right) - 1 \right], \quad (92)$$

Particle Losses	Dephasing model	Multimode $T \neq 0$
$ \psi(t)\rangle = \mathcal{N}^{1/2} e^{i\tilde{\phi}} \phi + \frac{\chi t}{2} \mathcal{D}\rangle$	$(\theta_a - \theta_b)(t) = (\theta_a - \theta_b)(0^+) - \chi t [2S_z + D]$	$(\theta_a - \theta_b)(t) = (\theta_a - \theta_b)(0^+) - \chi t [2S_z + D_{\text{th}}]$
\mathcal{D} from quantum jumps (77)	D from a dephasing Hamiltonian (15)	D_{th} from excited modes population (89)
$\xi^2(t) \underset{\rho g t / \hbar > 1}{\simeq} \frac{\langle \mathcal{D}^2 \rangle}{N}$	$\xi^2(t) \underset{\rho g t / \hbar > 1}{\simeq} \frac{\langle D^2 \rangle}{N}$	$\xi^2(t) \underset{\rho g t / \hbar > 1}{\simeq} \frac{\langle D_{\text{th}}^2 \rangle}{N}$
$\frac{\langle \mathcal{D}^2 \rangle}{N} = \frac{\gamma t}{3} = \frac{\epsilon_{\text{loss}}}{3}$	$\frac{\langle D^2 \rangle}{N} = \epsilon_{\text{noise}}$	$\frac{\langle D_{\text{th}}^2 \rangle}{N} = \sqrt{\rho a^2 F(k_B T / \rho g)} \underset{k_B T > \rho g}{\simeq} \epsilon_{\text{Bog}}$

TABLE I: Correspondence table among the different physical models. The results are valid in the thermodynamic limit and to first order in the small parameters ϵ_{loss} (69), ϵ_{noise} (16) and ϵ_{Bog} (87).

where now $n_k^{(0)}$ are Bose mean occupation numbers of Bogoliubov modes in state a before the pulse

$$n_k^{(0)} = \frac{1}{e^{\epsilon_k / k_B T} - 1}, \quad \epsilon_k = \sqrt{E_k(E_k + 2\rho g)}. \quad (93)$$

$s_k = U_k + V_k$ and $s_k^{(0)} = U_k^{(0)} + V_k^{(0)}$ where $U_k^{(0)}$ and $V_k^{(0)}$ are the Bogoliubov functions in internal state a before the pulse

$$U_k^{(0)} + V_k^{(0)} = \left(\frac{E_k}{E_k + 2\rho g} \right)^{1/4}; \quad E_k = \frac{\hbar^2 k^2}{2m}. \quad (94)$$

A consequence of (92) is that the squeezing divided by $\sqrt{\rho a^3}$ is an universal function of $k_B T / \rho g$.

C. Spin squeezing and non-condensed fraction

Within our treatment, valid for large N and $T \ll T_c$, we find that the best squeezing ξ_{min}^2 (92) is always lower than the before-pulse non-condensed fraction. This is shown in Fig.10.

Finally in Table IV A we can complete the correspondence table between dephasing noise, losses and non-zero temperature effects.

V. A FEW WORDS ABOUT EXPERIMENTS

Two recent experiments demonstrated spin squeezing in Bose-condensed bimodal condensates of rubidium atoms in internal states $|a\rangle = |F = 1, m_F = \mp 1\rangle$ and $|b\rangle = |F = 2, m_F = \pm 1\rangle$ [4, 6]. Due to the fact that the three scattering lengths characterizing the interactions between atoms are very close

$$g_{aa} \simeq g_{ab} \simeq g_{bb} \quad (95)$$

the effective two-mode nonlinearity χ in H_{nl} (8) is very small when the condensates a and b overlap spatially. This gives the possibility to *tune* the non-linearity [11] by either controlling the spatial overlap between the two species as done [6] or by using a Feshbach resonance changing the inter-species coupling constant g_{ab} as done in [4]. A fundamental source of decoherence in these experiments is two-body losses in the state $F = 2$. A theoretical analysis [11] shows that in typical experimental conditions these losses limit the squeezing to about $\xi_{\text{min}}^2 \simeq 6 \times 10^{-2}$. For cold samples this limit is above the limit imposed by non-zero temperature. In the case of [6] we could explain in detail the squeezing results using a zero-temperature model including spatial dynamics and including particle losses and technical noise (dephasing noise) as sources of decoherence, the latter being dominant [6, 18].

The perspective of studying experimentally the scaling of squeezing in a controlled decoherence environment, e.g. preparing the sample at different temperatures, is fascinating and challenging.

VI. CONCLUSIONS

We have considered a scheme to create spin squeezing using interactions in Bose-condensed gas with two internal states [2, 7, 8]. The squeezing is created dynamically after a $\pi/2$ pulse applied on the system initially at equilibrium in one internal state. We have reviewed the ultimate limits of this squeezing scheme imposed by particle losses and non-zero temperature based on our recent works [12] and [19] and we have extracted a simple physical picture of how decoherence acts in the system. An important result is that contrarily to the case without decoherence [2] the squeezing parameter minimized over time ξ_{min}^2 has a finite non-zero value in the thermody-

dynamic limit, that we determine analytically. Finally we have shown that the physics of spin squeezing in presence of losses or at non-zero temperature can be caught by a simple dephasing model (also considered in [16]) that we have solved exactly and studied in details.

Appendix A: Times t_{\min} and t'_η in the dephasing model

The exact solution (47)-(50) allows to determine how the best squeezing time t_{\min} diverges in the thermodynamic limit. We first found numerically that it diverges as $N^{1/4}$. We then introduce the rescaled time θ such that

$$\frac{\rho g}{\hbar} t = \theta N^{1/4}. \quad (\text{A1})$$

Expanding the functions $\cos^{N-2}(2\chi t)$ and $\exp[-2(\chi t)^2 \langle D^2 \rangle]$ up to terms $O(1/N)$ included in A; linearizing $\sin(\chi t)$ and expanding $\cos^{N-2}(\chi t)$ and $\exp[-(\chi t)^2 \langle D^2 \rangle / 2]$ up to terms $O(1/N^{1/2})$ included in B; and expanding $\cos^{N-1}(\chi t)$ and $\exp[-(\chi t)^2 \langle D^2 \rangle / 2]$ up to terms $O(1/N^{1/2})$ included in C, we obtain

$$\xi^2(t) = \frac{\epsilon_{\text{noise}}}{1 + \epsilon_{\text{noise}}} + \frac{1}{N^{1/2}} \left[\epsilon_{\text{noise}} \theta^2 + \frac{1}{\theta^2 (1 + \epsilon_{\text{noise}})^3} \right] + O\left(\frac{1}{N}\right). \quad (\text{A2})$$

By minimizing (A2) over θ one obtains

$$\begin{aligned} \frac{\rho g}{\hbar} t_{\min} &\stackrel{\text{lim. therm.}}{\sim} \left[\frac{N}{\epsilon_{\text{noise}} (1 + \epsilon_{\text{noise}})^3} \right]^{1/4}, \quad (\text{A3}) \\ \xi_{\min}^2 &\stackrel{\text{lim. therm.}}{=} \frac{\epsilon_{\text{noise}}}{1 + \epsilon_{\text{noise}}} + \frac{2}{N^{1/2}} \frac{\epsilon_{\text{noise}}^{1/2}}{(1 + \epsilon_{\text{noise}})^{3/2}} + O\left(\frac{1}{N}\right) \end{aligned} \quad (\text{A4})$$

With a similar technique we can determine the divergence of t'_η that is the second solution of equation (37) $t'_\eta > t_{\min}$. When $N \rightarrow \infty$, t'_η diverge as $N^{1/2}$. To calculate the prefactor we introduce again a rescaled time $\rho g t / \hbar = \theta' [N / (1 + \epsilon_{\text{noise}})]^{1/2}$ and take the large N limit in (47) to obtain

$$\xi^2(t) = e^{\theta'^2} \left[1 - \frac{1}{1 + \epsilon_{\text{noise}}} \frac{\theta'^2}{\sinh \theta'^2} \right] + O\left(\frac{1}{N}\right). \quad (\text{A5})$$

Solving the transcendental equation $(1 + \eta) \xi^2 = \xi_{\min}^2$ one finds the large N approximation to t'_η . For $\eta \ll 1$ and no constraint on the ratio $\eta / \epsilon_{\text{noise}}$, we obtain

$$\theta'^2 \simeq \frac{2\eta}{1 + \sqrt{1 + \frac{2\eta}{3\epsilon_{\text{noise}}}}}. \quad (\text{A6})$$

Appendix B: Calculation of $\langle \mathcal{D}^2 \rangle$ in the lossy model

From the definition of \mathcal{D} (77) and the expression of a quantum average (65) in the Monte Carlo wavefunction method, using the expression of the norm squared of $|\psi(t)\rangle$ of (76), we obtain

$$\begin{aligned} \langle \mathcal{D}^2 \rangle(t) &= e^{-\gamma N t} \sum_{k=1}^N \binom{N}{k} \gamma^k e^{k\gamma t} \int_0^t dt_1 \dots \int_0^t dt_k \\ &\frac{1}{2^k} \sum_{\eta_1, \dots, \eta_k = \pm 1} \left(\frac{1}{t} \sum_{i=1}^k \eta_i t_i \right)^2 \left(\prod_{i=1}^k e^{-\gamma t_i} \right). \end{aligned} \quad (\text{B1})$$

We have introduced the random variables $\eta_i = +1$ for $\epsilon_i = b$ and $\eta_i = -1$ for $\epsilon_i = a$, and we have used the fact that the integrand is a symmetric function of the jump times t_i to extend time integration from the ordered domain $0 < t_1 < \dots < t_k$ to the hypercube $[0, t]^k$ (also dividing by $k!$). The notation $\binom{N}{k}$ represents the usual binomial coefficient $N! / [k!(N-k)!]$. We first sum over the variables η_i :

$$\frac{1}{2^k} \sum_{\eta_1, \dots, \eta_k = \pm 1} \left(\sum_{i=1}^k \eta_i t_i \right)^2 = \sum_{i=1}^k t_i^2 \quad (\text{B2})$$

then we perform the temporal integration to obtain

$$\langle \mathcal{D}^2 \rangle = e^{-\gamma N t} \sum_{k=1}^N \binom{N}{k} k u^k \frac{I_2}{I_0}, \quad (\text{B3})$$

$$I_0 = \int_0^t dt_1 e^{-\gamma t_1} = \frac{1 - e^{-\gamma t}}{\gamma}, \quad (\text{B4})$$

$$\begin{aligned} I_2 &= \int_0^t dt_1 t_1^2 e^{-\gamma t_1} \\ &= \frac{1}{\gamma^3} \{ 2 - e^{-\gamma t} [2 + 2\gamma t + (\gamma t)^2] \}, \end{aligned} \quad (\text{B5})$$

$$u = \gamma e^{\gamma t} I_0 = e^{\gamma t} - 1. \quad (\text{B6})$$

Taking the derivative with respect to u of the binomial identity $\sum_{i=0}^k \binom{N}{i} u^i = (1+u)^N$, we get the final expression

$$\frac{\langle \mathcal{D}^2 \rangle}{N} = \frac{\gamma I_2}{t^2}. \quad (\text{B7})$$

Expanding I_2 for small γt gives as expected

$$\frac{\langle \mathcal{D}^2 \rangle}{N} \simeq \frac{1}{3} \gamma t. \quad (\text{B8})$$

- [2] Masahiro Kitagawa and Masahito Ueda. Squeezed spin states. *Phys. Rev. A*, 47(6):5138–5143, Jun 1993.
- [3] G. Santarelli, Ph. Laurent, P. Lemonde, A. Clairon, A. G. Mann, S. Chang, A. N. Luiten, and C. Salomon. Quantum projection noise in an atomic fountain: A high stability cesium frequency standard. *Phys. Rev. Lett.*, 82(23):4619–4622, Jun 1999.
- [4] C. Gross, T. Zibold, E. Nicklas, J. Esteve, and Oberthaler M.K. Nonlinear atom interferometer surpasses classical precision limit. *Nature*, 464:1165, 2010.
- [5] Ian D. Leroux, Monika H. Schleier-Smith, and Vladan Vuletić. Implementation of cavity squeezing of a collective atomic spin. *Phys. Rev. Lett.*, 104(7):073602, Feb 2010.
- [6] Riedel M.F., Boehi P., Li Yun, Hansch T.W., Sinatra A., and Treutlein P. Atom-chip-based generation of entanglement for quantum metrology. *Nature*, 464:1170, 2010.
- [7] Sorensen A., Duan L.M., Cirac J.I., and Zoller P. Many-particle entanglement with Bose-Einstein condensates. *Nature*, 409:63, 2001.
- [8] Uffe V. Poulsen and Klaus Mølmer. Positive-P simulations of spin squeezing in a two-component Bose condensate. *Phys. Rev. A*, 64(1):013616, Jun 2001.
- [9] Yvan Castin and Jean Dalibard. Relative phase of two Bose-Einstein condensates. *Phys. Rev. A*, 55:4330–4337, Jun 1997.
- [10] A. Sinatra and Y. Castin. Phase dynamics of Bose-Einstein condensates: Losses versus revivals. *Eur. Phys. Jour. B*, 4:247, 1998.
- [11] Li Yun, Treutlein P., Reichel J., and Sinatra A. Spin squeezing in a bimodal condensate: spatial dynamics and particle losses. *European Physical Journal B*, 68(3):365–381, 2009.
- [12] Yun Li, Y. Castin, and A. Sinatra. Optimum spin-squeezing in Bose-Einstein condensates with particle losses. *Phys. Rev. Lett.*, 100:210401, 2008.
- [13] Anders Søndberg Sørensen. Bogoliubov theory of entanglement in a Bose-Einstein condensate. *Phys. Rev. A*, 65(4):043610, Apr 2002.
- [14] P. Carruthers and Michael Martin Nieto. Phase and angle variables in quantum mechanics. *Rev. Mod. Phys.*, 40:411–440, Apr 1968.
- [15] E. M. Wright, T. Wong, M. J. Collett, S. M. Tan, and D. F. Walls. Collapses and revivals in the interference between two Bose-Einstein condensates formed in small atomic samples. *Phys. Rev. A*, 56(1):591–602, Jul 1997.
- [16] G. Ferrini, D. Spehner, A. Minguzzi, and F.W.J. Hekking. Effect of phase noise on useful quantum correlations in Bose Josephson junctions. *arXiv:1105.4495v1*.
- [17] K. Mølmer, Y. Castin, and J. Dalibard. A Monte-Carlo wave function method in quantum optics. *J. Opt. Soc. Am. B*, 10:524, 1993.
- [18] Yun Li. PhD Thesis at University Pierre et Marie Curie. <http://tel.archives-ouvertes.fr/tel-00506592/fr/>, 2010.
- [19] A. Sinatra, E. Witkowska, J.-C. Dornstetter, Yun Li, and Y. Castin. Limit of spin squeezing in finite-temperature Bose-Einstein condensates. *Phys. Rev. Lett.*, 107:060404, Aug 2011.
- [20] A. Sinatra, Y. Castin, and E. Witkowska. Nondiffusive phase spreading of a Bose-Einstein condensate at finite temperature. *Phys. Rev. A*, 75(3):033616, Mar 2007.
- [21] A. Sinatra, Y. Castin, and E. Witkowska. Coherence time of a Bose-Einstein condensate. *Phys. Rev. A*, 80(3):033614, Sep 2009.
- [22] Christophe Mora and Yvan Castin. Extension of bogoliubov theory to quasicondensates. *Phys. Rev. A*, 67:053615, May 2003.
- [23] In ^{87}Rb atoms this may be done by spatial separation of the spin states [6] or by Feshbach tuning of the a - b scattering length [4].
- [24] One could ask what would be the scaling of $\langle D^2 \rangle$ in the thermodynamic limit in case the dephasing would have a real physical origin. Let us consider for example an external random potential $\delta U(\mathbf{r})$ with zero mean, $\langle \delta U(\mathbf{r}) \rangle = 0$, that would induce an opposite energy shift for the two components: within the two-mode model, $\delta H_a = \int d^3r |\phi_a|^2 \delta U(\mathbf{r}) a^\dagger a$ and $\delta H_b = - \int d^3r |\phi_b|^2 \delta U(\mathbf{r}) b^\dagger b$. In this case, from equations (15) and (10) one has $\langle (gD)^2 \rangle = \int d^3r \int d^3r' \langle \delta U(\mathbf{r}) \delta U(\mathbf{r}') \rangle$. The scaling (16) would then correspond to a fluctuating potential $\delta U(\mathbf{r})$ that has short-range spatial correlations so that the correlation function $\langle \delta U(\mathbf{r}) \delta U(\mathbf{r}') \rangle = f(|\mathbf{r} - \mathbf{r}'|)$ is integrable. On the other hand, a uniform fluctuating potential δU would correspond to $\langle D^2 \rangle$ scaling as N^2 . One might finally imagine a fluctuating potential $\delta U(\mathbf{r})$ that is non-zero only in a finite region of space. In this case one would get $\langle D^2 \rangle$ independent of N . This is what we call the “weak dephasing limit”. We treat this limit in subsection II C.
- [25] We have verified numerically that this approximation is excellent provided that the lost fraction of particles is small.

0,06

0,05

z

y

$$S_x = N/2$$

x

